environmental sciences proceedings

MDPI

Proceeding Paper

Split-Window Algorithm for Land Surface Temperature Retrieval from Joint Polar-Orbiting Satellite System JPSS-2/NOAA-21

Fatima Zahrae Rhziel, Mohammed Lahraoua and Naoufal Raissouni

National School for Applied Sciences of Tetouan, University Abdelmalek Essaadi, Remote Sensing, Systems and Telecommunications research unit; fatimazahrae.rhziel@etu.uae.ac.ma (F.Z.R.); naoufal.raissouni.ensa@gmail.com (N.R.)
* Correspondence: m_lahraoua@yahoo.fr

Abstract: Land Surface Temperature (LST) plays a pivotal role in the dynamic exchange of energy between the Earth's surface and the atmosphere. This research centers on the assessment of LST from satellite data acquired by the Joint Polar-orbiting Satellite System (JPSS), specifically JPSS-2/NOAA-21, employing an innovative Split Window Algorithm (SWA). Atmospheric Water Vapor Content (WVC) and surface emissivity are the two main input variables in the split-window technique. Therefore, the Moderate Resolution Transmittance Code version 4.0 (MODTRAN 4.0) was used to simulate WVC and atmospheric transmittance. The performance of the SWA was rigorously assessed against standard atmospheric conditions, revealing its capacity to achieve an LST retrieval accuracy of 1.4 Kelvin (K), even in the presence of various errors. . Moreover, the LST retrieval algorithm was validated using ground-truth data sets from two Australian sites and the RMSE value was 1.71 K. The achieved results demonstrate the algorithm's capability to provide accurate LST estimation for NOAA-21 satellite data.

Keywords: land surface temperature; split window algorithm; VIIRS and JPSS-2/NOAA-21

1. Introduction

Land Surface Temperature (LST) is a necessary parameter with a profound impact on the physical processes of land surfaces, influencing a range of phenomena from local to global scales. It drives the outgoing longwave radiation and turbulent heat fluxes at the interface between the Earth's surface and the atmosphere. Consequently, LST routinely applied in various fields such as evapotranspiration [1–4], the estimation of soil moisture [5–8], and environmental studies [9–12]. Furthermore, the International Geosphere and Biosphere Program (IGBP) [13] consider LST as one of the high priority parameters.

According to one of the sustainable development goals (SDGs) promoted by the United Nations, the increase in the earth's surface temperature is regarded as a major phenomenon [14]. Hence, it is crucial to monitor this dilemma in order to evaluate the rapid variations of LST spatially and temporally in the globe for vast geographic areas. The only way to measure LST on a worldwide scale is through remote sensing satellite data, which makes this conceivable [15].

The estimation of LSTs from TIR satellites data requires two primary parameters: emissivity and atmospheric corrections [16,17]. Over the course of several decades, researchers have dedicated their efforts to refining algorithms for deriving LST from TIR remote sensing data, using a range of approaches to deal with emissivity and atmospheric effects. Among these algorithms, the split-window (SW) technique stands out, as it directly mitigates atmospheric distortions by leveraging the brightness temperature (BT)

Citation: To be added by editorial staff during production.

Academic Editor: Firstname Lastname

Published: date

from two adjacent TIR channels at the top of the atmosphere. This method is frequently employed for producing operational LST products [18–21]

The satellite NOAA-21, designated Joint Polar Satellite System JPSS-2 prior to launch [22], was launched on 10 November 2022 [22] by the National Oceanic and Atmospheric Administration (NOAA). Its primary objective is to furnish comprehensive global environmental data, encompassing insights into weather patterns, atmospheric dynamics, and various environmental indicators. A scanning radiometer sensor onboard NOAA-21 called VIIRS gathers visible and infrared imagery as well as radiometric measurements of the land, atmosphere, and oceans. Interestingly, two of the 22 spectral bands on VIIRS, which range in wavelength from 0.4 to 12.5 m, are thermal infrared channels that will be used for LST retrieval.

In this study, SW algorithm was developed for JPSS-2, validation and comparison with ground-based measurements verified the algorithm's efficacy in providing accurate and reliable land surface temperature estimates over diverse landscapes and climatic conditions.

2. Methodology

2.1. Split-Window Algorithm for LST Retrieval

The SW technique, which is based on the differential absorption in two neighboring infrared channels, was initially developed for calculating Sea Surface Temperature (SST) from satellite observations. Then, it was expanded to estimating land surface temperature. In this study, the emissivity and water vapor effects have been taken into consideration by using the SW-LST algorithm structure described by Sobrino and Raissouni [23] to retrieve LST from VIIRS NOAA-21 data. This algorithm is written as follows:

$$LST = T_{15} + c_1(T_{15} - T_{16}) + c_2(T_{15} - T_{16})^2 + c_0 + (c_3 + c_4 W)(1-\varepsilon) + (c_5 + c_6 W)\Delta\varepsilon \quad (1)$$

where Ts is the earth surface temperature (in K), T_{15} and T_{16} are the at-sensor brightness temperatures (in K) of VIIRS NOAA-21, ε = (ε15 + ε16)/2 presents the mean effective emissivity, Δε= (ε15 − ε16) is the difference between the emissivities of VIIRS channels M15 and M16, W (g. cm^{-2}) is the total atmospheric water vapor column, and c_k (k= 0, 1 … 6) are the SW algorithm coefficients.

2.2. VIIRS Sensor Characteristics

Visible Infrared Imaging Radiometer Suite (VIIRS) is a whiskbroom radiometer designed for use onboard S-NPP, NOAA-20, NOAA-21, and future JPSS series satellites. The carachteristics of the thermal infrared M15 and M16 bands that have been used in the SWA for LST retrieval are presented in table 1 and figure 1.

Table 1. The split window M15 and M16 Bands characteristics of VIIRS sensor.

JPSS -VIIRS Band	Wavelength (µm)	Bandwidth (µm)	Spatial Resolution (m)
M15	10.763	10.26-11.26	750
M16	12.013	11.54-12.49	750

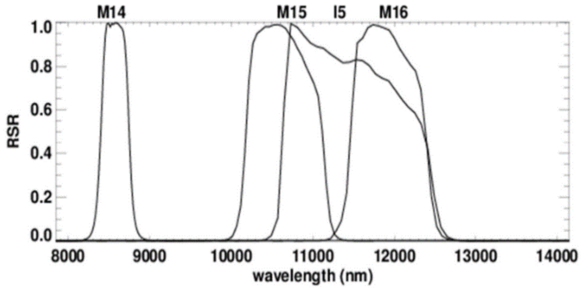

Figure 1. Relative spectral response function of VIIRS channels M15 and M16 onboard NOAA-21.

2.3. MODTRAN 4.0 Simulations

In order to determine the atmospheric parameters (downwelling and upwelling atmospheric radiances and atmospheric transmettance), the radiative transfer model (RTM) MODTRAN was used. The atmospheric profiles were extracted from Thermodynamic Initial Guess Retrieval (TIGR) database [24]. To better characterize surface variations, the calculations were done over a vast gradient of temperatures, T-5, T, T+5, T+10, and T+20 (taken into account that T is the initial boundary layer temperature of the profiles). 100 emissivities of various types of surfaces were taken from the Advanced Spaceborne Thermal Emission Reflection Radiometer (ASTER) spectral [25]. Furthermore, five different view angles (0º, 10º, 20º, 30º and 40º) and 54 atmospheric water vapor (W) values at nadir (variying between 0.15 g.cm^{-2} and 4.65 g.cm^{-2}) were used in the simulation in order to consider the viewing angle and atmospheric water vapor effects. Therefore, 135000 simulation data was composed.

2.4. Numerical Coefficients and Sensitivity Analysis

We conducted a sensitivity analysis based on the error theory to assess the performance of the SW algorithm and the impact of the possible errors in LST estimation. The sensitivity analysis is given by the following equation:

$$\delta_{\text{Total}}(T_s) = \sqrt{\delta_{\text{alg}}^2 + \delta_{\text{NE}\Delta\text{E}}^2 + \delta_{\varepsilon}^2 + \delta_{\text{W}}^2} \tag{2}$$

where δ_{alg} is the algorithm's standard deviation, $\delta_{NE\Delta T}$, δ_W and δ_ε are the impacts on total error due to uncertainties of sensor temperatures, atmospheric water vapor and land surface emissivity, respectively. $\delta_{NE\Delta T}$, δ_W and δ_ε are expressed by the following equations:

$$\delta_{\text{NE}\Delta\text{E}} = \sqrt{\left(\frac{\partial T_s}{\partial T_{15}}\right)^2 e^2(T_{15}) + \left(\frac{\partial T_s}{\partial T_{16}}\right)^2 e^2(T_{16})} \tag{3}$$

$$\delta_W = \left(\frac{\partial T_s}{\partial W}\right) e(W) \tag{4}$$

$$\delta_\varepsilon = \sqrt{\left(\frac{\partial T_s}{\partial \varepsilon_{15}}\right)^2 e^2(\varepsilon_{15}) + \left(\frac{\partial T_s}{\partial \varepsilon_{16}}\right)^2 e^2(\varepsilon_{16})} \tag{5}$$

Thus, we assume that both the brightness temperature errors of M15 and M16 channels $e(T_{15}) = e(T_{16}) = 0.05$ K or 0.01 K, the emissivity errors in VIIRS channels M15 and M16 $e(\varepsilon 15) = e(\varepsilon 16)$ are 0.01 or 0.005 [26] and the atmospheric water vapor content can be considered as e(W) = 0.5 g.cm^{-2} [27]

3. Results and Discussion

3.1. Sensitivity Analysis

The SW coefficients (c0 to c6) of the developed SWA for LST estimation from NOAA-21 satellite are presented in Table 2.

Table 2. Split-Window algorithm coefficients (c_0 to c_6) for JPSS-2/NOAA-21 satellites.

Satellite	λ_{ieff}	λ_{jeff}	C_0	C_1	C_2	C_3	C_4	C_5	C_6
NOAA-20	10.763	12.013	–0.16	1.330	0.230	58.1	–0.57	–112	8.84

The results of sensitivity analysis are shown in Table 3. The emissivity uncertainty is about 1.26 K and 0,63 K for and for e(ε4) = e(ε5) = 1 % and e(ε15) = e(ε16) = 0.5% successively. The total LST uncertainty δTotal(Ts), is about 1.67 K considering e(ε15) = e(ε16) = 1 % and it is less than 1.26 K for e(ε15) = e(ε16) = 0.5 %. Therefore, the uncertainties in emissivity has insignificant effect on the LST estimation. Thus, an accurate knowledge of surface is required.

Table 3. The sensitivity analysis of the parameters influencing LST estimation onboard NOAA-21.

Satellite	λ_{eff} (μm)	λ_{eff} (μm)	R	δ_{alg} (K)	$\delta_{NE\Delta T}$ (K)	δ_{ε} (1%)	δ_{ε} (0.5%)	δ_W (K)	$\delta_{Total}(T_s)$ (1%)	$\delta_{Total}(T_s)$ (0.5%)
NOAA-21	10.654	11.934	0.93	1.07	0.22	1.26	0.63	0.02	1.67	1.26

3.2. LST Validation

The accuracy of the proposed SWA for LST retrieval from VIIRS/NOAA-21, is also evaluated using ground truth data sets from the Hay and Walpeup sites [28].

Figure 2 presents the LST retrieved from NOAA-21 satellite using the developed split window algorithm and the in-situ LST ground data from two Australian sites (Hay and Walpeup) as well as the correlation coefficient R, bias, standard deviation differences (SDV) and Root Mean Square Error (RMSE). The results show that the split window algorithm onboard NOAA-21 can estimate LST with a bias of 0.97 K, a standard deviation differences of 1.31 K, and an RMSE of less than 1.71 K for the Hay and Walpeup sites measurements, confirming the algorithm's accuracy in LST retrieval.

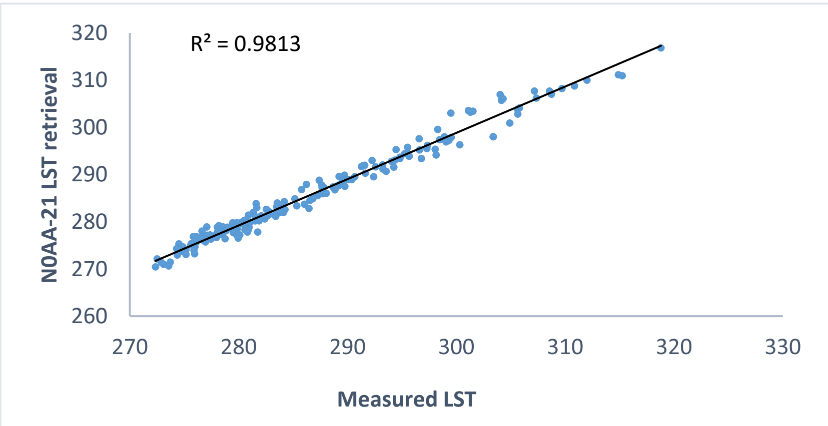

Figure 2. Validation of NOAA-21 split window algorithm using the ground truth data set of [28].

4. Conclusion

An alternate split-window technique for LST estimation from NOAA-21 satellite data was proposed in this study. The algorithm coefficients were obtained from the simulation dataset of atmospheric profiles. To assess the performance of the SW- LST method, a sensitivity analysis was performed.

The derived LST's accuracy was validated using ground truth data sets from two Australian sites. The recovered LST shows a good fitting with the in situ LST at both sites. The bias and RMSE are respectively 0.97 and 1.71 K. This indicates that this algorithm offers an alternate and feasible method for retrieving LST using NOAA-21 satellite data. Nonetheless, more LST validation under various atmospheric conditions and surface types is required to adequately evaluate the efficacy of this approach.

Supplementary Materials: The following supporting information can be downloaded at: www.mdpi.com/xxx/s1, Video S1 and Video S2, are respectively the monthly calculated surface-height anomalies derived from ICESat-2 over three-month periods. Video S1 covers the downstream lakes of the RIS, while Video S2 covers the upstream lakes of the RIS.

Funding:

Institutional Review Board Statement:

Informed Consent Statement:

Data Availability Statement:.

Conflicts of Interest:

References

1. Olioso. A. H. Chauki. D. Couraul. and J. P. Wigneron.: Estimation of evapotran spiration and photosynthesis by assimilation of remote sensing data into SVAT models. Remote Sensing of Environment. vol. 68. pp. 341-356. (1999)
2. V. V. Serafini.: Estimation of the evapotranspiration using surface and satellite data. International Journal of Remote Sensing. vol. 8. pp. 1547-1562. (1987)
3. N. Bussieres. P. Y. T. Louie. and W. Hogg.: Progress Report on the Implementation of an Algorithm to Estimate Regional Evapotranspiration Using Satellite Data. Applications of remote sensing in hydrology. Saskaton Saskatchewan. (1990)
4. L. Zhang. R. Lemeur. and J. P. Gouthorbe.: A one-layer resistance model for estimating regional evapotranspiration using remote sensing data. Agriculture and Forest Meteorology. vol. 77. pp. 241-261. (1995)
5. T. J. Schmugge.: Remote sensing of surface soil moisture. Journal of Applied Meteorology. vol. 17. pp. 1549-1557. (1978)
6. J. C. Price.: The potential of Remotely Sensed Thermal Infrared data to Infer Surface Soil Moisture and Evaporation. Water Resources. vol. 16. pp. 787-795. (1990)
7. D. C. A. Uitdewilligen. W. P. Kustas. and P. J. van Oevelen.: Estimating surface soil moisture with the scanning low frequency microwave radiometer (SLFMR) during the Southern Great Plains 1997 (SGP97) hydrology experiment. Physics and Chemistry of the Earth. Parts A/B/C. vol. 28. no. 1-3. pp. 41-51. (2003)
8. J. Santanello. C. D. Peters-Lidard. M. E. Garcia. D. M. Mocko. M. A. Tischler. M. S. Moran. and D. P. Thoma.: Using remotely-sensed estimates of soil moisture to infer soil texture and hydraulic properties across a semi-arid watershed. Remote Sensing of Environment. vol. 110. no. 1. pp. 79-97. (Sept.2007)
9. Arnfield, A. J.: Two decades of urban climate research: a review of turbulence, exchanges of energy and water, and the urban heat island. International Journal of Climatology, 23, 1–26 (2003)
10. Bastiaanssen, W. G. M., Menenti, M., Feddes, R. A., & Holtslag, A. A. M.: A remote sensing surface energy balance algorithm for land (SEBAL). 1. Formulation. Journal of Hydrology, 212, 198–212 (1998)
11. Kogan, F. N.: Operational space technology for global vegetation assessment. Bulletin of the American Meteorological Society, 82, 1949–1964 (2001)
12. Kalma, J. D., McVicar, T. R., & McCabe,M. F.: Estimating land surface evaporation: A review of methods using remotely sensed surface temperature data. Surveys in Geophysics, 29, 421–469(2008)
13. Townshend, J. R. G., Justice, C. O., Skole, D., Malingreau, J. P., Cihlar, J., Teillet, P., et al.: The 1 km resolution global data set: needs of the International Geosphere Biosphere Programme. International Journal of Remote Sensing, 15, 3417–3441 (1994)
14. United Nations, The Sustainable Development Goals Report 2019, New York. Available online: https://unstats.un.org/sdgs/report/2019/The-Sustainable-Development-Goals-Report-2019.pdf (accessed on 13 September 2023).
15. Z. Li et al.: Satellite-derived land surface temperature: current status and perspec tives. Remote Sens. Environ. 131,14–37 (2013)
16. Li, Z.-L., & Becker, F. (1993). Feasibility of land surface temperature and emissivity de- termination from AVHRR data. Remote Sensing of Environment, 43,67–85.
17. Vidal, A. (1991). Atmospheric and emissivity correction of land surface temperature measured from satellite using ground measurements or satellite data. International Journal ofRemote Sensing, 12, 2449–2460.

18. Yu, Y.; Tarpley, D.; Privette, J.L.; Raja, M.K.R.V.; Vinnikov, K.; Xu, H. Developing algorithm for operational GOES-R land surface temperature product. IEEE Trans. Geosci. Remote Sens. 2009, 47, 936–951.
19. Caselles, V.; Coll, C.; Valor, E. Land surface temperature determination in the whole Hapex Sahell area from AVHRR data. Int. J. Remote Sens. 1997, 18, 1009–1027. [CrossRef]
20. Trigo, I.; Freitas, S.; Bioucas-Dias, J.; Barroso, C.; Monteiro, I.; Viterbo, P. Algorithm Theoretical Basis Document for Land Surface Temperature (LST) Products: LSA-001(MLST), LSA-050 (MLST-R). 2017. Available online: https://landsaf.ipma.pt/en/products/land-surface-temperature/lst/ (accessed on 20 September 2023).
21. Wan, Z. MODIS Land-Surface Temperature Algorithm Basis Document (LST ATBD): Version 3.3. 1999. Available online: https://modis.gsfc.nasa.gov/data/atbd/atbd_mod11.pdf (accessed on 20 September 2023).
22. https://www.nesdis.noaa.gov/news/jpss-2-has-new-name-noaa-21 (accessed on 22 September 2023).
23. J. A. Sobrino and N. Raissouni. "Toward remote sensing methods for land cover dynamic monitoring. Application to Morocco." International Journal of Remote Sensing. vol. 20. no. 2. pp. 353-366. 2000
24. N. A. Scott and A. Chedin. "A fast line by line method for atmospheric absorption computations: The authomatized atmospheric absorption atlas." Journal of Meteorology. vol. 20. pp. 802-812. 1981.
25. S. J. Hook. "The ASTER Spectral Library." Pasadena. CA: Jet Propulsion Lab. [Online]. vol. Available at http://speclib.jpl.nasa.gov/ 1999.
26. Caselles, V., E. Valor, C. Coll, and E. Rubio. 1997. "Thermal Band Selection for the PRISM Instrument. 1. Analysis of Emissivity-Temperature Separation Algorithms." Journal of Geophysical Research 102 (D10): 11145–11164. doi:10.1029/97JD00344.
27. Vey, S., R. Dietrich, A. Rülke, M. Fritsche, P. Steigenberger, and M. Rothacher. 2010. "Validation of Precipitable Water Vapor within the NCEP/DOE Reanalysis Using Global GPS Observations from One Decade." Journal of Climate 23 (7): 1675–1695. doi:10.1175/2009JCLI2787.1.
28. A. J. Prata. "Land surface temperatures derived from the advanced very high resolution radiometer and the along-track scanning radiometer 2: experimental results and validation of AVHRR algorithms." Journal of Geophysical Research. vol. 99. pp. 13025-13058. 1994.